

ISOTOPES ACCUMULATION IN THE THERMAL COLUMN OF TRIGA REACTOR

C. IORGULIS, D. DIACONU, D. GUGIU, R. CSABA

Institute for Nuclear Research Pitesti, Romania, daniela.diaconu@nuclear.ro

ABSTRACT

The correlation of impurity observed in the virgin graphite and radionuclide content and activities measured in the irradiated graphite needs to know the irradiated history. This is a challenging process if impurity content and irradiation conditions are not accurately known. This is the case of the irradiated graphite in the thermal column of Institute for Nuclear Research Pitesti (INR)14 MW TRIGA reactor. To overcome incomplete impurity content and the unknown position in the column of the measured irradiated graphite available for characterisation and comparison, a set of preliminary simulations were performed. Following Eu152/Eu154 ration they allowed the estimation of an impurity content and irradiation conditions leading to measured activities. Based on these data the radio-isotope accumulation in different positions in the thermal column was predicted. Modelling performed by INR used advanced prediction packages (e.g. WIMS, MCNP ORIGEN-S from Scale 5) to assess the isotopic content of MTR graphite types with irradiation history specific for a TRIGA research reactor. Some certain calculations points from the column were selected in order to model the burnup and isotopes productions using ORIGEN from SCALE code system.

Introduction

The thermal column of TRIGA reactor consists in a block of 96 rectangular bricks of graphite encased in Aluminum. The thermal column is placed on a stainless steel frame fixed in the reactor pool, in the northern part of the steady state zone [1]. It was built up in 1985 and it was mainly used for several experiments in thermal flux conditions.

The graphite was imported in the '50s from a UK producer but documents of origin were lost. No information on its characteristics and especially on the impurity content could be found.

Since its installation in the reactor pool, few changes in the column structure consisting in replacement of some bricks occurred, but no track of these changes exist. Only one brick was extracted and dismantled in 2000 without a reference to its position in the thermal column. Samples collected from this brick were used for radionuclide content measurements.

Characteristics of the graphite used in TRIGA thermal column

TRIGA thermal column design

An aluminum encased graphite brick is a parallelepiped with a square section of 14.3 cm length and 71 cm high. The whole thermal column size having 12 rows of 8 bricks is 172x114x71cm. The graphite brick is composed by graphite pieces with different geometries as shown in **Figure 1**.

The graphite used in TRIGA thermal column is sintered graphite with a density of 1.72 g/cm³. The total mass of graphite in a brick is 24.97 Kg and the whole column weights 2.447Kg.

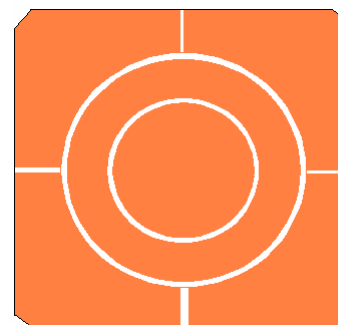


Figure 1
Geometry of a graphite brick

Impurity content of the virgin graphite

The assessment of isotope accumulation in the irradiated graphite using computer codes simulating neutron reactions requires:

- irradiation history
- impurity content

Impurity analysis was experimentally determined under Carbowaste project in WP 3.2 by energy-dispersion X-rays spectroscopy (SEM/EDX) and X-rays fluorescence (XRF). The XRF measurements on different virgin graphite samples led to impurity content as presented in **Table 1**.

Table 1 Impurity content in virgin graphite measured by XRF

Element	Percent wt (%)	Standard error
C	99.87 – 99.95	
Na	0.0420 - 0.0628	0.0033
Ba	0.0037 - 0.0229	0.0033
Si	0.0127 - 0.0173	0.001
Mg	0.0245 - 0.0070	0.0009
Cl	0.0063 - 0.0059	0.0007
Ca	0.0038 - 0.0082	0.0005
S	0.0020 - 0.0031	0.0003
Th	0 - 0.0023	0.0009
Dy	0 - 0.0021	0.0008
K	0.0012 - 0.0018	0.0005
Al	0.0011 - 0.109	0.0003
Mo	0 - 0.0025	0.0007
Sn	0 - 0.0232	0.0012
Fe	0 - 0.014	0.0007
Cr	0 - 0.0011	0.0001
P	0 - 0.0011	0.0003

But, due to the limits of the investigation techniques, the above impurity content is not complete. Configuration of the X Rays Fluorescence Spectrometer ARL ADVANTA'X IntelliPower™ Series does not allow determination of elements lighter than Na, while EDX configuration of the scanning electronic microscope TESCAN VEGA II LMU (even reliable in the identification of impurity elements) does not

allow determination of elements lighter than C. Consequently, no data on Li content could be obtained and concentration of N achieved by EDX should be considered with large uncertainties (**Table 2**).

Table 2 EDS measurements on N content in virgin graphite

Element	Percent wt (%)	Standard error
N	0.01	0.01

Detection limit is another parameter limiting the accurate measurement of impurity content by these techniques even for heavy elements. Therefore EDX and XRF measurements did not reveal the presence of Co and Eu, but both were found in the irradiated graphite from the thermal column.

Gamma spectroscopy measurements (**Table 3**) on irradiated samples showed the presence of Co and Eu at activities corresponding to very low concentration (ppb), much under the XRF or EDS sensitivity limit.

Table 3 Average activity of Co and Eu in a irradiated graphite sample

Radionuclide	Activity (Bq/g)
Co60	52.35 ± 2
Eu152	1333.20 ± 24
Eu154	67.85 ± 4

Characteristics

During its Irradiation s functioning in TRIGA reactor, the thermal column was irradiated at an average power of 10MW. The neutrons have a strong variation along column both in energy and flux. Therefore, the flux of fast neutrons decreases from 10^{11} nv in the edge next to the reactor core to 10^6 nv in the center. Correspondingly, the thermal neutrons flux has also a significant decrease from 10^{13} nv to 10^8 nv.

This large variation in flux composition excludes an average approach of isotopes accumulation in the thermal column of TRIGA reactor, since neutron reactions occurring in the graphite depends on the neutron energy and consequently on the position in the column.

Radionuclide content measured in the thermal column of TRIGA reactor

Combining gamma scanning and beta spectroscopy, a large number of graphite samples were measured for the characterization of the radionuclide content. Techniques and methods available in IRN allowed the determination of Co-60, Cs-134 and Cs 137, Eu 152 and Eu 154, C-14 and H-3 activities.

Table 4 gives a synthesis of the radionuclide activities measured in 2011 in this graphite brick. These values will be use to compare the codes predictions to the real activity data. The samples used in these measurements were collected from different pieces composing the graphite brick extracted from the thermal column in 2000.

Table 4 Radionuclides activity measured in a graphite brick

Radionuclide	Measured activity (Bq/g)
H3	0.7÷2E+04
C14	0.8÷1.9E+03
Co60	1.7-6.9E+01
Eu152	0.5÷1.9E+03
Eu154	0.3÷1.2E+02

Model of C-14 accumulation in MTR

Modeling tools for radionuclide content assessment

The tools used in the modeling of radionuclide content accumulation in the graphite irradiated in the thermal column of TRIGA reactor were:

- WIMS (Cell transport code) for cross section generation [2]
- DFA (System of Tridimensional Core codes with Burn-up Loop) for flux and power distribution calculation
- ORIGEN-S From Scale 5 (Burn-up code) for nuclide densities and activities evaluation [3]
- Origen’s (LWR) Library

Hypothesis and model

The burn-up calculation has been carried out considering 10MW average reactor power using real energy history released as presented in **Figure 2**.

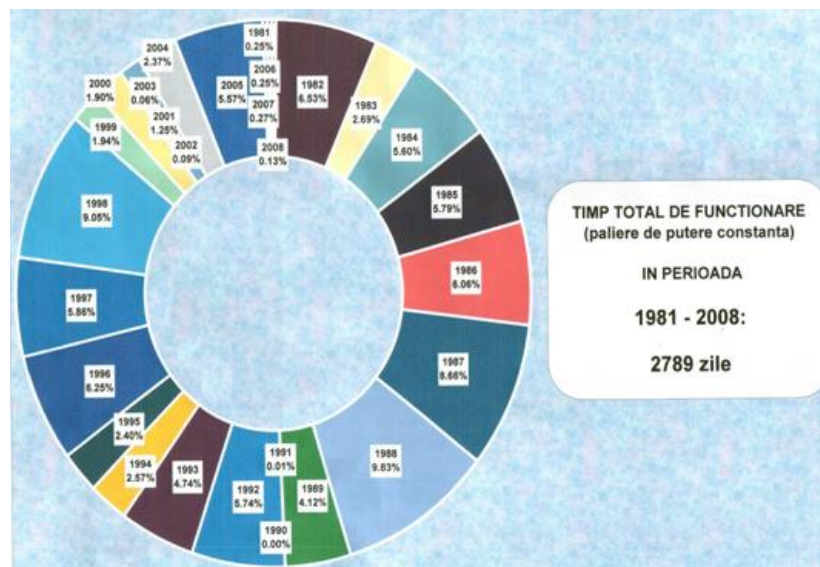


Figure 2 TRIGA Released Energy History used for ORIGEN Calculations

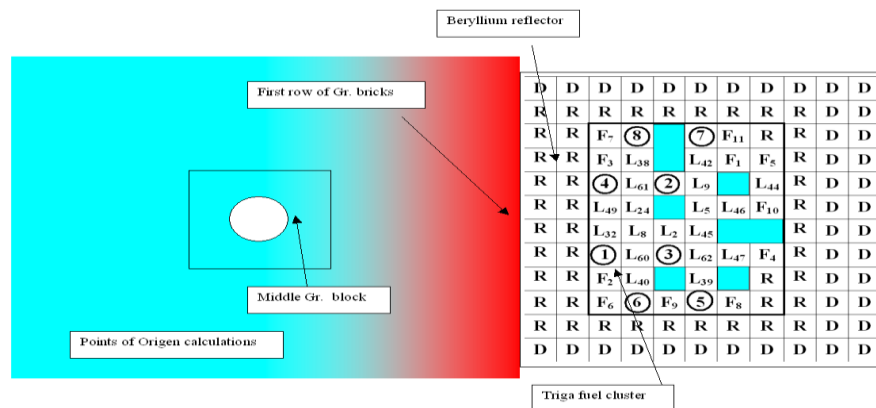


Figure 3 General geometry layout used for neutronic calculations

The thermal column was modeled according to its real geometry and configuration of the TRIGA INR reactor (**Figure 3**):

- Column size: 172x114x71cm³
- Number of graphite bricks: 96 (12 rows of 8 bricks)
- Graphite block size: 14.3x14.3x71 cm.
- Distance from the reactor core: 25 cm
- Beryllium wall width: 17.78 cm

Input data

In order to calculate the radionuclides accumulated in the graphite during the operation of TRIGA reactor, the following input data have been considered:

- Column installation date: 1985
- Irradiation time and power: equivalent of 10 years at 10 MW
- Times outside the column: 5 and respectively 10 years

Preliminary simulations

The assessment with a reasonable low uncertainty of the radionuclide inventory for the irradiated graphite needs as pre-requisite information accurate impurity content and exact irradiation history. This is not the case for the graphite from the thermal column of TRIGA reactor whose impurity content and their amount are affected by large uncertainties. Contrary, the recording data on reactor operation allow the simulation of a quite accurate irradiation history.

In order to minimize uncertainties associated to the impurity content, preliminary simulations were performed to calculate the radionuclides activity starting with the an impurity content experimentally determined by XRF on one of the graphite sample (**Table 5**) and using an irradiation flux with average characteristics:

- Flux Th: 6.90E+10nv
- Flux Epi: 1.10E+8nv
- Flux Fast: 4.0E+6nv

Table 5 Impurity content considered for preliminary simulation

Impurity (by XRF)	Na	Ba	Si	Mg	Cl	Ca	Sx	Al	K	P	Th	Dy
Concentration (g/Kg C)	0.628	0.229	0.173	0.07	0.063	0.038	0.031	0.023	0.011	0.018	0.02	0.011

The radioactive elements resulted from the activation and fission reactions of C and impurity content are listed in **Table 6**.

Table 6 Predicted radionuclide content in irradiated graphite from TRIGA thermal column for the measured impurity content

Radionuclide	Activity (Ci /kg)		
	at discharge	5y after	10 y after
H 3	5.81E-18	4.39E-18	3.32E-18
Be10	6.36E-13	6.36E-13	6.36E-13
C14	2.72E-06	2.72E-06	2.72E-06
Si32	2.02E-16	1.98E-16	1.94E-16

P32	1.02E-04	1.98E-16	1.94E-16
S35	6.59E-04	3.48E-10	1.83E-16
Cl36	8.41E-07	8.41E-07	8.41E-07
Ar39	4.43E-11	4.37E-11	4.32E-11
K40	1.12E-11	1.12E-11	1.12E-11
Ca41	1.56E-08	1.56E-08	1.56E-08
Ca45	1.94E-05	8.58E-09	3.79E-12
Sc46	5.34E-09	1.49E-15	4.14E-22
Cs134	5.44E-10	1.01E-10	1.89E-11
Cs135	2.32E-19	2.32E-19	2.32E-19
Ba133	5.15E-06	3.70E-06	2.66E-06
Eu152	5.88E-15	4.54E-15	3.50E-15
Eu154	2.83E-13	1.89E-13	1.26E-13
Eu155	2.36E-15	1.12E-15	5.37E-16
Gd153	3.33E-10	1.77E-12	9.41E-15
Tb157	5.47E-08	5.34E-08	5.22E-08
Tb160	1.04E-09	2.63E-17	6.64E-25
Dy159	3.05E-06	4.79E-10	7.54E-14
Ho166m	2.67E-09	2.66E-09	2.65E-09

The comparison of activities predicted at 10 years after the extraction of the graphite brick from the thermal column with the activities values measured on the irradiated samples at the same time (**Table 7**) led to the following conclusions:

- Large amount of H-3 experimentally measured can be justified only if activation of light elements (as Li) at impurity level is considered
- C-14 activity predicted from C-13 activation is also underestimated compared to the measured values, suggesting that activation of N adsorbed on the particle surface brings an important contribution and must be considered.
- Eu152 and Eu154 activities resulted by fission of impurity as Th or Dy do not match neither the activities measured on the graphite block, nor the ratio Eu152/Eu154, indicating that Eu as impurity, even at ppb level has to be considered.
- Co 60 is not predicted by simulation if Co as impurity is neglected.

Table 7 Predicted vs. measured radionuclides activity for XRF impurity content

Radionuclide	Predicted Activity (Bq/g)	Measured activity (Bq/g)
H3	1.23E-10	0.7÷2E+04
C14	1.01E+02	0.8÷1.9E+03
Co60	-	1.7÷6.9E+01
Eu152	1.30E-07	0.5÷1.9E+03
Eu154	4.66E-06	0.3÷1.2E+02

Based on these conclusions, new runs have been performed considering the presence of Li, N, Co and Eu as impurity.

Since concentration values are not available as direct measurements, an indirect calculation starting from the measured radionuclide activity on graphite sampled from the thermal column and the irradiation history could be an option. But, as position in the thermal column of the measured graphite is not known (is uncertain), neutron flux is not available.

To overcome this apparently vicious circle, the code was run for different positions in the column following Eu152/Eu154 ratio to match as much as possible the measured values ranging between 12 and 18 (**Figure 4**). The closest ratio obtained was 10.2 Adding N concentration determined by EDX (0.01% wt), simulations confirmed that the optimum irradiation flux leading both to measured C-14 activity (10^3 Bq/g) and a reasonable Eu152/Eu154 ratio should have the following flux spectrum:

- Flux Th: 1.7e11nv
- Flux Epi: 9.5e8nv
- Flux Fast: 8.2e7nv

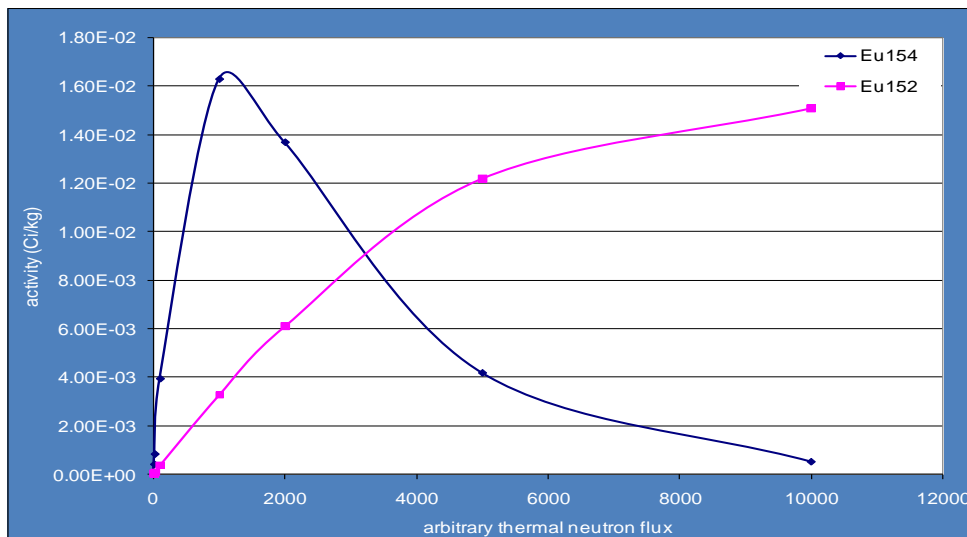


Figure 4 Variation of Eu152 and Eu154 activity as function of thermal neutron flux

For this neutrons flux Li, Eu and Co concentrations were estimated based on the neutron activation approach (**Table 8**).

The values of the neutrons flux place the graphite brick used in the irradiated graphite characterization in the third row of the column from the reactor core.

Table 8 Impurity assessed by inverse method

Impurity	Eu	Li	Co
Concentration (g/Kg C)	7.00E-06	6.20E-05	3.00E-06
Comments	Estimated from neutron activation		

Radionuclide assessment

Having the impurity content of the graphite obtained by XRF measurements (**Table 1**) plus N measured by EDS, and Eu, Li and Co calculated based on neutron activation (**Table 8**), radionuclide accumulation in different locations of the thermal columns has been calculated in the following cases:

Case A:

- *neutron flux*: - determined as optimum flux matching C-14 activity and Eu152/Eu154 ratio

Case B:

- *neutron flux*: corresponding to the geometrical centre of the column:
 - Flux Th: 5. e10 nv;
 - Flux Epi: 0.9e8 nv
 - Flux Fast: 3.2e6 nv

Case C:

- *neutron flux*: corresponding to the centre of the first row near to the active (maximum flux)
 - Flux Th: 2e13 nv;
 - Flux Epi: 2.6e12nv
 - Flux Fast: 3.79e11nv

Predictions of radionuclide content and activities**Case A**

The radioactive elements resulted from the activation and fission reactions of C and the assumed impurity are listed in **Table 9**. For the radionuclide listed in **Table 10**, the predicted activities fall in the range of the measured values, excepting Eu154 which is overestimated. Also, the ratio Eu152/Eu154 (10.2) predicted by simulations is lower than the value obtained from the measured activities which ranges between 12 and 18.

Table 9 Case A. Predicted radionuclide content for the measured sample location (thermal column's third row)

radionuclide	Activity (Ci /kg)		
	at discharge	after 5y	after 10y
H 3	4.61E-04	3.48E-04	2.63E-04
Be10	1.49E-12	1.49E-12	1.49E-12
C14	2.60E-05	2.59E-05	2.59E-05
Si32	1.23E-15	1.21E-15	1.18E-15
P32	2.53E-04	1.21E-15	1.18E-15
S35	1.63E-03	8.58E-10	4.53E-16
Cl36	2.07E-06	2.07E-06	2.07E-06
Ar39	1.58E-10	1.56E-10	1.54E-10
K40	1.38E-11	1.38E-11	1.38E-11
Ca41	3.86E-08	3.86E-08	3.86E-08
Ca45	4.79E-05	2.12E-08	9.36E-12
Sc46	3.25E-08	9.06E-15	2.52E-21
Co60	2.68E-06	1.39E-06	7.20E-07
Ni63	7.44E-20	7.19E-20	6.94E-20
Cs134	3.39E-09	6.33E-10	1.18E-10
Cs135	3.56E-18	3.56E-18	3.56E-18
Ba133	1.27E-05	9.13E-06	6.57E-06
Sm151	1.60E-16	1.54E-16	1.48E-16
Eu152	7.38E-05	5.69E-05	4.39E-05
Eu154	9.64E-06	6.44E-06	4.30E-06
Eu155	3.09E-07	1.47E-07	7.02E-08
Gd152	5.09E-18	5.67E-18	6.12E-18

Gd153	3.67E-06	1.95E-08	1.04E-10
Tb157	1.44E-07	1.40E-07	1.37E-07
Tb160	6.68E-09	1.68E-16	4.25E-24
Dy159	7.57E-06	1.19E-09	1.87E-13
Ho166m	1.66E-08	1.66E-08	1.65E-08

Table 10 Case A. Comparison with measured radionuclides activity

Radionuclide	Predicted Activity Measured activity	
	(Bq/g)	(Bq/g)
H 3	0.973E+04	0.7÷2E+04
C14	0.958E+03	0.8÷1.9E+03
Co60	2.66E+01	1.7÷6.9E+01
Eu152	1.62E+03	0.5÷1.9E+03
Eu154	1.59E+02	0.3÷1.2E+02

Case B

Smaller neutrons flux corresponding to the centre of the thermal column leads to the same radionuclide content (excepting Ni-63) but to a lower activity, generally 10 times smaller (**Table 11**).

Table 11 Case B. Predicted radionuclide content in column centre

Radionuclide	Activity (Ci /kg)			Radionuclide	Activity (Ci /kg)		
	at discharge	after 5 y	after 10 y		at discharge	after 5 y	after 10 y
H 3	1.36E-04	1.03E-04	7.76E-05	Cs134	2.85E-10	5.32E-11	9.92E-12
Be10	1.64E-13	1.64E-13	1.64E-13	Cs135	8.81E-20	8.81E-20	8.81E-20
C14	7.62E-06	7.62E-06	7.61E-06	Ba133	3.73E-06	2.68E-06	1.93E-06
Si32	1.06E-16	1.04E-16	1.02E-16	Sm151	1.54E-18	1.48E-18	1.43E-18
P32	7.42E-05	1.04E-16	1.02E-16	Eu152	2.46E-05	1.89E-05	1.46E-05
S35	4.78E-04	2.52E-10	1.33E-16	Eu154	2.85E-06	1.90E-06	1.27E-06
Cl36	6.09E-07	6.09E-07	6.09E-07	Eu155	2.73E-08	1.30E-08	6.23E-09
Ar39	1.53E-11	1.51E-11	1.50E-11	Gd152	1.66E-18	1.86E-18	2.01E-18
K40	1.07E-11	1.07E-11	1.07E-11	Gd153	3.45E-07	1.84E-09	9.76E-12
Ca41	1.13E-08	1.13E-08	1.13E-08	Tb157	3.96E-08	3.87E-08	3.78E-08
Ca45	1.41E-05	6.22E-09	2.75E-12	Tb160	5.48E-10	1.38E-17	3.49E-25
Sc46	2.81E-09	7.81E-16	2.18E-22	Dy159	2.21E-06	3.47E-10	5.46E-14
Co60	7.83E-07	4.05E-07	2.11E-07	Ho166m	1.41E-09	1.40E-09	1.40E-09

Case C

The maximum neutrons flux determines a richer content of radionuclides and higher activities (**Table 12**).

Table 12 Case C. Predicted radionuclide content in the first row of the thermal column

Radionuclide	Activity (Ci /kg)			Radionuclide	Activity (Ci /kg)		
	at discharge	after 5 y	after 10 y		at discharge	after 5 y	after 10 y
H3	1.84E-02	1.39E-02	1.05E-02	Ba133	1.47E-03	1.06E-03	7.59E-04
Be10	6.15E-08	6.15E-08	6.15E-08	Ba137m	3.96E-04	1.39E-13	1.24E-13

C14	3.04E-03	3.04E-03	3.03E-03	Ce142	1.07E-19	1.07E-19	1.07E-19
Si32	1.74E-11	1.71E-11	1.67E-11	Ce144	9.39E-17	1.11E-18	1.31E-20
P32	3.02E-02	1.71E-11	1.67E-11	Pr144	2.62E-14	1.09E-18	1.29E-20
S35	1.66E-01	8.74E-08	4.61E-14	Pm147	9.72E-18	2.66E-18	7.11E-19
Cl36	2.22E-04	2.22E-04	2.22E-04	Sm151	7.79E-13	7.49E-13	7.21E-13
Ar37	7.02E-04	1.48E-19	3.12E-35	Eu152	1.09E-07	8.40E-08	6.48E-08
Ar39	1.87E-06	1.85E-06	1.83E-06	Eu154	1.66E-04	1.11E-04	7.41E-05
Ar40	1.10E-14	9.92E-15	8.93E-15	Eu155	1.14E-04	5.45E-05	2.60E-05
K40	4.88E-10	4.88E-10	4.88E-10	Gd152	4.11E-19	4.12E-19	4.13E-19
K42	7.88E-03	9.92E-15	8.93E-15	Gd153	9.16E-05	4.87E-07	2.59E-09
Ca41	4.52E-06	4.52E-06	4.52E-06	Tb157	1.39E-05	1.36E-05	1.33E-05
Ca45	5.61E-03	2.48E-06	1.10E-09	Tb160	6.97E-05	1.76E-12	4.43E-20
Sc46	4.29E-04	1.20E-10	3.33E-17	Dy159	7.61E-04	1.20E-07	1.88E-11
Co60	2.88E-04	1.50E-04	7.75E-05	Ho166m	4.69E-05	4.68E-05	4.67E-05
Ni63	1.31E-11	1.27E-11	1.22E-11	Tm170	5.24E-06	2.80E-10	1.49E-14
Zn65	3.75E-18	2.10E-20	1.17E-22	Tm171	4.53E-08	7.46E-09	1.23E-09
Cs134	3.93E-05	7.33E-06	1.37E-06				
Cs135	4.94E-12	4.94E-12	4.94E-12				
Cs137	1.66E-13	1.48E-13	1.31E-13				

Table 13 shows a variation covering magnitude orders in activity of the most important radionuclides along the column. This table groups also the most active radioisotopes defining the inventory of the thermal column installed in a TRIGA 14MW reactor.

Table 13 Radionuclides activities for different positions in the thermal column

Radionuclide	Predicted Activity (Bq/g)			Measured activity (Bq/g)
	Column centre	Sample location	First row	
H3	2.87E+03	0.973E+04	3.89E+05	0.7÷2 E+04
C14	2.82E+02	0.958E+03	1.12E+05	0.8÷1.9 E+03
Co60	7.79E+00	2.66E+01	2.87E+03	1.7-6.9 E+01
Eu152	5.40E+02	1.62E+03	2.40E+00	0.5÷1.9 E+03
Eu154	4.70E+01	1.59E+02	2.74E+03	0.3÷1.0 E+02
Eu155	2.31E-01	2.60E+00	9.62E+02	-
Ba133	7.14E+01	2.43E+02	2.81E+04	-
Cl36	2.25E+01	7.66E+01	8.21E+03	-
Ni63	-	2.57E-12	4.51E-04	-
Ho166m	5.18E-02	6.11E-01	1.73E+03	-
Cs134	3.67E-04	4.37E-03	5.07E+01	

Conclusions

1. Uncertainties on impurity content have an important impact on the predicted activities of radionuclides.
2. The simulation of the radionuclide accumulation in a thermal column pointed out that:

- only very small content of Li explains high activity of H-3 but experimental evidences are needed to prove it.
 - only the presence of Eu as impurity, even at very low level, can explain the measured activities and Eu152/Eu154 ratio
 - C-14 activity is sensitive to N content and future measurements are needed to confirm the value used in simulation.
3. Radionuclide content after irradiation during TRIGA reactor operation depends on the position in the thermal column due to the variation of the irradiation flux.
 4. Due to the strong decrease of the irradiated flux, the radionuclides activity in MTR irradiated graphite has a large variability along the thermal column.
 5. The most important radio-isotopes in the thermal column inventory predicted by the models are H-3, C-14, Co-60, Cl-36, Eu-152, Eu-154, Eu-155, Ba-133, Ho-166m. Their activity decreases two to three magnitude orders only in the half towards the reactor core.
 6. While thermal column model developed under this study can predict accurately the value of the flux along the thermal column, position of the graphite block used in experimental measurements is unknown. Moreover, it could hasn't had during all irradiation period the same position inside the thermal column. This can explain the differences between the predicted and measured values in this study.
 7. Integrating the activities predicted by the models over the entire thermal column for the total operation period, the total inventory can be estimated. Future works will be done to define a less uncertain impurity content and therefore to assess the total inventory of the irradiated graphite in TRIGA reactor.

References

- [1] Roth, Csaba. *Dispozitiv coloana termica*. IRNE. 1986. Project. 660-0
- [2] K.Kovalska, S-*WIMS User's manual*
- [3] O.Hermann, R. Westfall, Origen : Scale system module to calculate fuel depletion and associated radiation source terms

III. SUSTAINABLE DEVELOPMENT